

Stable Radicals

Twisted Diarylnitroxides: An Efficient Route for Radical Stabilization

Oleg A. Levitskiy,^[a] Dmitry B. Eremin,^[b] Alexey V. Bogdanov,^[a] and
Tatiana V. Magdesieva*^[a]

Abstract: New strategy for the molecular design of stable diarylnitroxides was elaborated based on the insertion of a bulky substituent into the *ortho*-position of the phenyl ring thus disturbing its conjugation with the radical center. A series of new twisted diaryl nitroxides with *tert*-butyl and trifluoromethyl substituents in different positions and combinations was obtained and fully characterized. Electron spin resonance (ESR) and density functional theory (DFT) studies confirmed that the *ortho*-substituted phenyl ring is removed from the conjugation; the

O–N–C–C torsion angle was shown to be dependent not only on the bulkiness of the *ortho*-substituent, but it is also influenced by the electron-donating or electron-withdrawing ability of the substituents in both phenyl rings. These nitroxides constitute the first examples of stable diarylnitroxides with a vacant *para*-position on the phenyl ring. The new approach will broaden the scope of available stable diarylnitroxyl radicals, which are practically important.

Introduction

Stable *N,N*-disubstituted NO radicals, namely nitroxides, are of considerable interest for theoretical research and practical applications. They are widely used as spin and redox traps,^[1,2] antioxidants,^[3–6] redox-active electrode materials for energy conversion and storage systems,^[7–10] regulators in radical polymerization processes,^[11,12] and catalysts.^[13–17] The most widely investigated are dialkyl nitroxides, foremost, TEMPO (2,2,6,6-tetramethylpiperidine-1-oxyl) and its derivatives.^[2]

However, diarylnitroxides are much less investigated. Only a very limited number of stable diarylnitroxyls can be found in literature.^[18–21] Previously, diarylnitroxyls were not considered as promising candidates for stable radical species since the spin density is delocalized over the *ortho*- and *para*-positions of aromatic rings, thus providing additional reaction centers and decreasing the stability. It has been shown^[22] that the main decay channel for aryl nitroxides in solution is radical transformations involving the *para*-position of the phenyl ring, which leads to quinoid-type structures (see below). In the solid state, bi-, tri-, and polyradical species, formed from aryl nitroxides coupled through the *m*-phenylene units, are used as building blocks for organic magnetic materials.^[23–26] In all diarylnitroxides, which are relatively stable in solution, the *para*-positions of the aromatic rings are blocked with the appropriate substituents to prevent subsequent transformations.^[22] This substantially limits

the scope of stable radicals available. Meanwhile, diarylnitroxides are more favorable than alkyl derivatives for further functionalization of the molecule aimed at fine-tuning of the redox-properties required for each particular application.

An alternative route to achieve radical stabilization might be the insertion of a bulky substituent into the *ortho*-position of the phenyl ring, thus disturbing its conjugation with the radical center. However, this approach has not been probed yet. In this paper we demonstrate the possibility of obtaining stable diarylnitroxides with a vacant *para*-position. New *ortho*-substituted diarylnitroxides, devoid of a *para*-substituent, should be nonetheless stable as a result of steric interactions, which force the *ortho*-substituted aryl to be twisted from the N–O plane, with the consequent inhibition of the resonance stabilization.

The first examples of diarylnitroxides containing *tert*-butyl and trifluoromethyl groups in *ortho*-position and in various combinations, which are stable in the solid state and in solution, are described. The twisted structure of the new compounds was supported by electron spin resonance (ESR) and density functional theory (DFT) studies. Stability is a crucial point in the evaluation of the practical application of new nitroxides as redox-active electrode materials for energy conversion and storage systems.^[27] This new approach will broaden the scope of available stable diarylnitroxyl radicals, which are practically important.

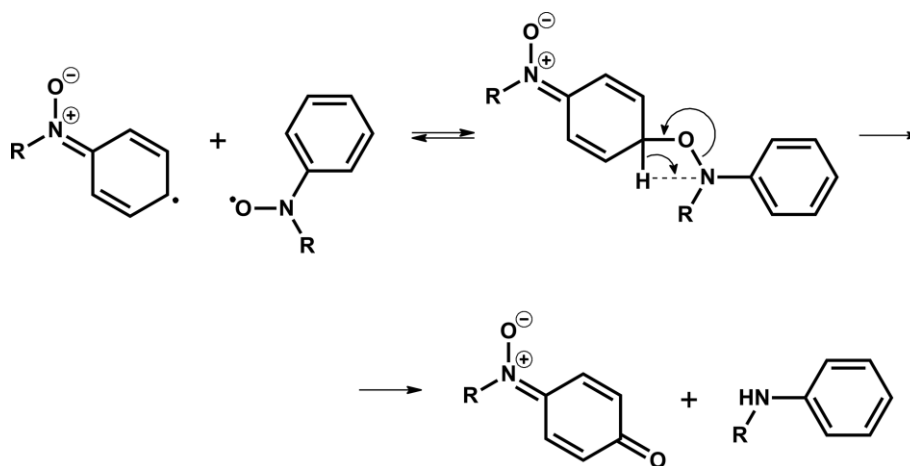
Results and Discussion

Diarylnitroxides can be obtained through oxidation of diarylamines by using H₂O₂/Na₂WO₄ or *m*-chloroperbenzoic acid.^[1,2] Diarylamines (see the previous paper^[28]) containing *ortho-tert*-butyl and trifluoromethyl groups were used as precursors for the corresponding nitroxides (Table 1).

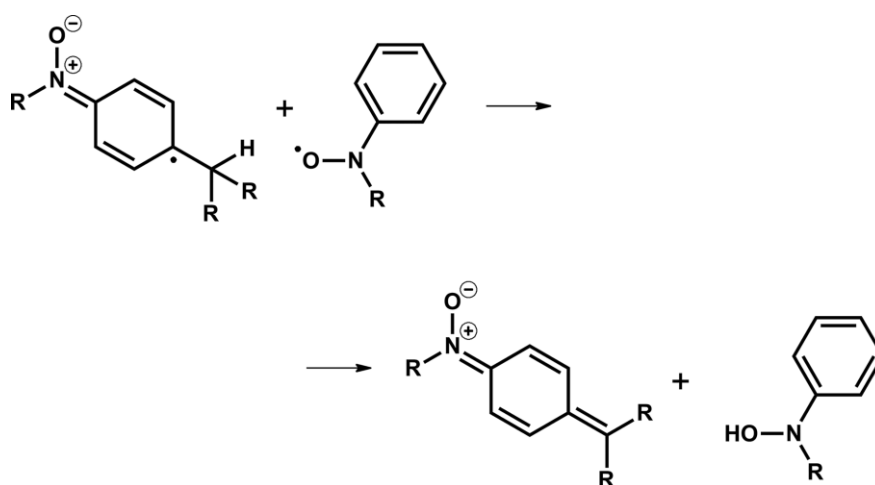
[a] Lomonosov Moscow State University, Chemistry Department,
Leninskie Gory 1/3, Moscow 119991, Russia
E-mail: tvm@org.chem.msu.ru
<http://www.chem.msu.ru/>

[b] Zelinsky Institute of Organic Chemistry Russian Academy of Sciences,
Leninsky Prospect 47, Moscow, Russia

Supporting information for this article is available on the WWW under
<https://doi.org/10.1002/ejoc.201700947>.



Scheme 1. Unwanted radical coupling via *para*-position of the arene ring.



Scheme 2. Main route for decomposition of diarylnitroxides with *para*-substituents with α -hydrogen atoms.

Table 1. Oxidation of amines to nitroxides.

	R ¹	R ²	Method	Yield [%]
1	<i>p</i> -tBu	<i>p</i> -tBu	a	70
2	<i>o</i> -tBu	<i>p</i> -tBu	a	45
3	<i>o</i> -tBu	<i>o</i> -tBu	b	10
4	<i>p</i> -CF ₃	<i>p</i> -tBu	a	29
5	<i>o</i> -CF ₃	<i>p</i> -CF ₃	b	25
6	<i>o</i> -CF ₃	<i>p</i> -tBu	b	31
7	<i>o</i> -tBu	<i>p</i> -CF ₃	b	41

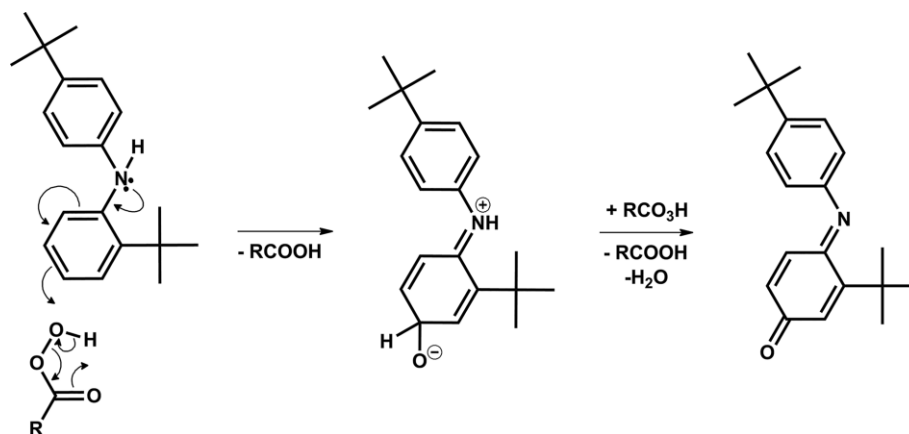
The selection of the starting diarylamines has several reasons. The substituents should be sufficiently bulky, to twist the phenyl ring from the conjugation with the N–O plane and to prevent the possible attack of the radical NO center of the one molecule to the *para*-position of the other molecule bearing a sufficient spin density (Scheme 1).^[22]

Only substituents without α -hydrogen atoms are suitable to suppress the other unwanted reaction channel (Scheme 2).^[22]

Finally, the chosen substituents exhibit the opposite electronic properties (tBu is an electron donor whereas CF₃ is an acceptor), which allows estimating the influence of this parameter on the nitroxide stability (e.g., hydrogen-atom abstraction ability and other side reactions).

Synthesis of the Nitroxides

Oxidation of 4,4'-bis(*tert*-butylphenyl)amine was performed with H₂O₂/Na₂WO₄ in boiling methanol, as it has been previously reported.^[29] For the oxidation of unsymmetrical 2,4'-bis(*tert*-butylphenyl)amine, several oxidants were tested. The best results were obtained by using H₂O₂ in boiling methanol in the presence of Na₂WO₄ (45 % yield). The oxidation with *m*-chloroperbenzoic acid in ether provided the targeted 2,4'-bis(*tert*-butylphenyl)nitroxide in much lower yield (19 %). The oxidation was initially performed at –15 °C but after 10 min, the temperature was gradually increased, and the reaction mixture was stirred for 2 h at room temperature. The unsymmetrical 2,4'-bis(*tert*-butylphenyl)nitroxyl radical was obtained as red crystals, and its identity was proved by ESI-HRMS (see the Experimental Section).



Scheme 3. Side reaction in 2,4'-bis(*tert*-butylphenyl)amine oxidation with mCPBA.

HPLC-MS analysis of the reaction mixture revealed, besides the targeted nitroxide, the presence of a by-product (ca. 10 %) corresponding to the compound of the quinoid type. The ^1H NMR spectrum of the mixture (see the Supporting Information, p. S4) exhibits the signals of two non-equivalent *tert*-butyl groups (1.59 and 1.49 ppm); the signals of the *para*-substituted phenyl ring (AA'BB' spin system signals at $\delta = 7.56$ and 6.91 ppm) and a set of signals corresponding to the substituted 1,4-quinoid ring (two doublets at $\delta = 7.21$ and 6.55 ppm and singlet at $\delta = 6.73$ ppm, Scheme 3). The formation of this by-product [supported also by CI-MS (see the Supporting Information, p. S3) data] in the course of the amine oxidation is an interesting observation, which is in line with the main idea of our investigation. This is an indication that a certain excess of π -electron density is still located at the *para*-position in spite of the presence of the bulky *ortho*-substituent in close vicinity to the amino group, which might influence the conjugation. The increased electron density in the *para*-position provokes an alternative oxidation route through attack of the peroxo-compound at the vacant *para*-position, which yields the minor by-product.

The NO group, which is more bulky than the NH group, significantly increases the O–N–C–C torsion angle and the rotation barrier of the *ortho*-substituted ring resulting in a decrease in the conjugation and stabilization of the NO radical due to almost negligible spin density in the *para*-position. This becomes evident from the DFT-optimized structures as well as from the ESR data (see below).

Oxidation of sterically demanding 2,2'-bis(*tert*-butylphenyl)amine, in which the lone pair of the N atom is shielded by the bulky substituents, was performed by using *m*-chloroperbenzoic acid which could be expected to provide less steric hindrance as compared to Na_2WO_4 . The reaction was extremely slow; K after a reaction time of three days, the starting colorless solution of the amine precursor turned pale red. The solution was evaporated, and the excess of the oxidant and the formed *m*-chlorobenzoic acid were separated by washings with toluene. After subsequent evaporation of the toluene solution, the residue was purified by column chromatography. The targeted 2,2'-bis(*tert*-butylphenyl)nitroxide was isolated (10 %) and characterized by HRMS and ESR methods.

Oxidation of CF_3 -containing amines is impeded due to the presence of the electron-withdrawing group. Oxidation of 4-*tert*-butyl-4'-trifluoromethyl-diphenylamine was performed with $\text{H}_2\text{O}_2/\text{Na}_2\text{WO}_4$ in boiling methanol. After 15 h of heating, the corresponding nitroxide was obtained in 29 % yield. The oxidation of the isomeric 4-*tert*-butyl-2'-trifluoromethyl-diphenylamine by using the same oxidant was not successful; no radical was obtained after three days of reflux. Therefore, the stronger oxidant (mCPBA) was used for obtaining the nitroxide radical from 4-,2'-bis(trifluoromethylphenyl)amine. The reaction mixture containing the amine and mCPBA in chloroform solution was heated for 5 h at 40 °C. The corresponding 4-,2'-bis(trifluoromethylphenyl)nitroxide was isolated in 25 % yield.

All radicals were characterized by HRMS and ESR methods (see the Experimental Section and the Supporting Information).

The purity of the isolated radical species was proven by the ESR through spin counting, to determine their spin concentration of the nitroxide samples.

ESR Characterization

Experimental and DFT-simulated spectra for all nitroxides under discussion were obtained. Computed and experimental data are in good agreement; the mean square deviation is 0.05 G. Based on the previously reported data,^[30] which demonstrated that of B1LYP functional is preferential over B3LYP for nitroxides, providing reasonable agreement of computed and experimental constants, the B1LYP functional with cc-pVDZ basis set was selected. The commonly used PWP functional with EPR-II basis set for ESR computations gave huge difference in a_{N} values; the accuracy for the a_{H} values were in the same range as the values previously obtained by using B1LYP (see the Supporting Information).

Comparative ESR investigation of isomeric 2,4'-, 2,2'-, and 4,4'-bis(*tert*-butylphenyl)nitroxides was performed revealing the influence of the steric bulkiness on the hyperfine constant values. The series of unsymmetrical *t*Bu and CF_3 -substituted nitroxides demonstrates the additional influence of the electronic effects. The ESR spectra obtained are given in Figure 1.

The ESR spectra of all nitroxides exhibit a triplet signal due to the spin splitting on the N atom. Besides, an additional split-

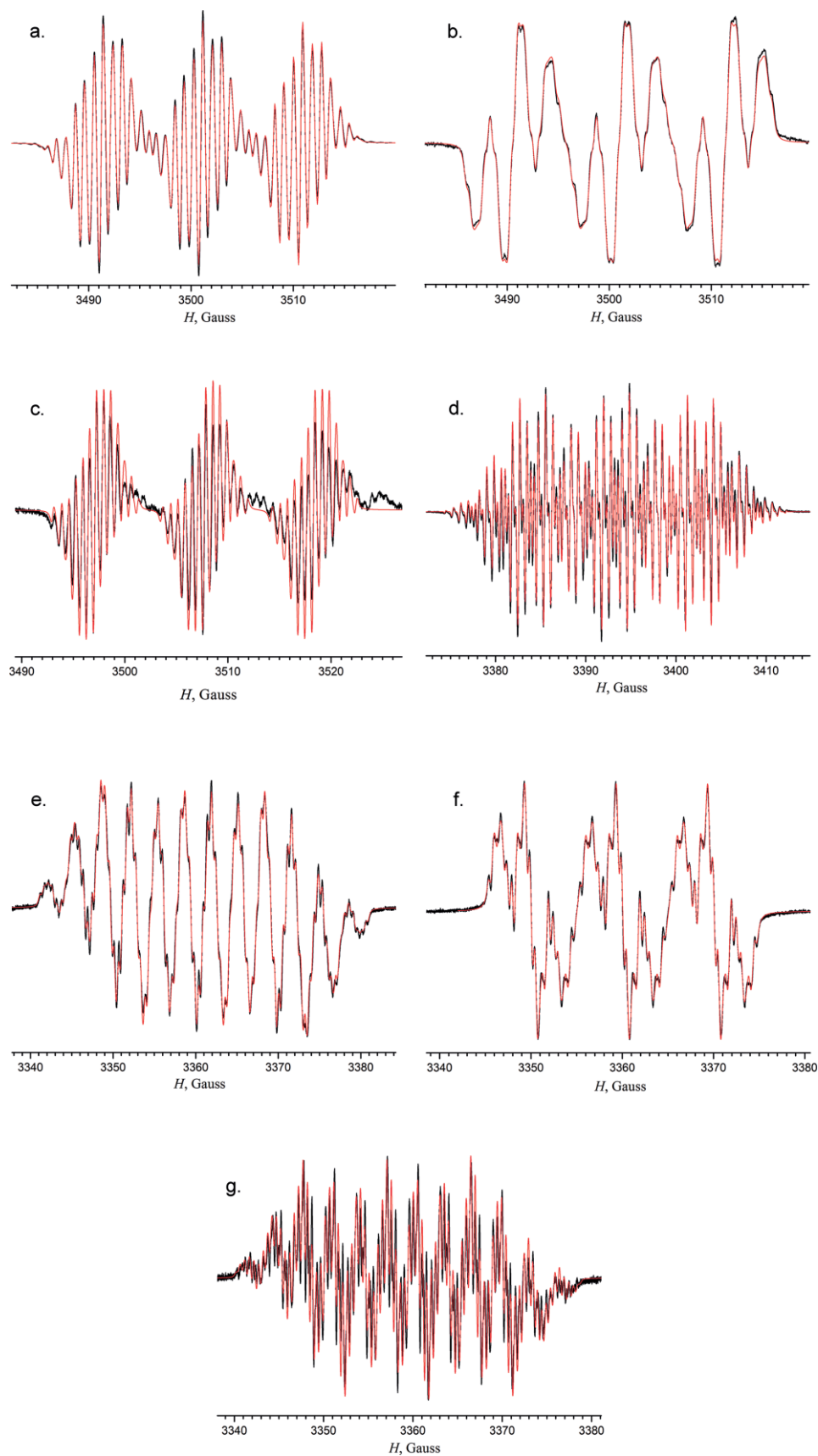


Figure 1. Experimental (black line) and simulated (red line) ESR spectra for 4,4'-bis(*tert*-butylphenyl)nitroxide (a); 2,4'-bis(*tert*-butylphenyl)nitroxide (b); 2,2'-bis(*tert*-butylphenyl)nitroxide (c); 4-(trifluoromethylphenyl)-4'-(*tert*-butylphenyl)nitroxide (d); 4-(trifluoromethylphenyl)-2'-(*tert*-butylphenyl)nitroxide (e); 2-(trifluoromethylphenyl)-4'-(*tert*-butylphenyl)nitroxide (f); 2,4'-bis(trifluoromethylphenyl)nitroxide (g).

ting of each triplet component is observed, which is dependent on the type of the substituent and its position. Experimental and simulated ESR spectra are in good agreement.

For three isomeric bis(*tert*-butylphenyl)nitroxides, additional splitting on the aromatic protons is observed. Digital simulation showed that the spectral pattern observed for 2,4'-bis(*tert*-butylphenyl)nitroxide is consistent with the spin splitting on the N atom as well as on two pairs of equivalent protons. This means that the spin density in this radical is delocalized over only one phenyl ring, which gives rise to the spin coupling on two *ortho*- and two *meta*-protons ($a_N = 10.34$ G, $a_H = 2.65$ G (*ortho*) and 0.88 G (*meta*), see Table 2). Hence, the other phenyl ring, which contains the *ortho-tert*-butyl group is removed from the conjugation plane with the nitroxyl radical center. The decrease in the conjugation chain (one ring in conjugation instead of two) is the reason for the observed increase in the spin splitting constants as compared to that for the 4,4'-bis(*tert*-butylphenyl)nitroxyl radical [see Table 2 and previously reported data, $a_N = 9.9$ G, $a_H = 1.86$ G (*ortho*) and 0.9 G (*meta*)^[29]]. The maximal *hfcc* value with the ¹⁴N nucleus is observed in case

of 2,2'-bis(*tert*-butylphenyl)nitroxide (Table 2), which indicates poor delocalization of the spin density over both phenyl rings.

For comparison, the ESR data previously obtained for the unsubstituted diphenylnitroxide are also inserted in Table 2. As can be expected, *g*-factor, a_N , and a_H *hfcc* are very close to our results obtained for planar 4,4'-bis(*tert*-butylphenyl)nitroxide radical.

The ESR spectra for trifluoromethylated diarylnitroxides are more complicated due to additional splitting on the fluorine atoms. The $a(F)$ constants are sensitive to the location of the CF₃ group. In case of the *ortho*-CF₃ group, the phenyl ring is partially removed from the conjugation with the NO radical center, and the *hfcc* with the F nucleus are much lower than that for the *para*-CF₃-substituent (0.16 G and 3.43 G, respectively, see Table 2).

The *hfcc* values are also influenced by the electronic properties of the substituents in the phenyl rings. Thus, the $a(N)$ values for 2,4'-bis(*tert*-butylphenyl)nitroxide and for 2-*t*Bu,4'-CF₃-diphenylnitroxide are sufficiently different (10.34 G and 9.7 G, re-

Table 2. *g*-Values and hyperfine spin coupling constants with ¹⁴N, ¹H, and ¹⁹F nucleus for the new nitroxides.

Radical	<i>g</i> -value	$a(N)$, G	DFT-calculated $a(N)$, G	$a(H)$, G	DFT-calculated $a(H)$, G	$a(F)$, G	DFT-calculated $a(F)$, G
4,4'- <i>t</i> Bu	2.00586	9.74	9.53	1.81 (2 H) 0.91 (2 H)	2.01 (2 H _{<i>ortho</i>}) 1.08 (2 H _{<i>meta</i>})	–	
2,4'- <i>t</i> Bu	2.00580	10.34	10.55	2.65 (2 H) 0.88 (2 H) 0.66 (1 H) 0.50 (1 H) 0.43 (1 H)	2.81 (2 H _{<i>ortho</i>}) 1.30 (2 H _{<i>meta</i>}) 0.56 (1 H _{<i>meta</i>}) 0.47 (1 H _{<i>ortho</i>}) 0.36 (1 H _{<i>para</i>})	–	
2,2'- <i>t</i> Bu	2.00621	10.59	11.59	1.40 (2 H) 1.21 (2 H) 0.82 (2 H) 0.67 (2 H)	1.27 (2 H _{<i>ortho</i>}) 0.90 (2 H _{<i>meta</i>}) 1.36 (2 H _{<i>para</i>}) 0.89 (2 H _{<i>meta</i>})	–	
4- <i>t</i> Bu-4'-CF ₃	2.00595	9.29	9.26	2.86 (2 H) 0.88 (2 H) 0.82 (2 H) 0.74 (2 H)	2.30 (2 H _{<i>meta</i>} vs. CF ₃) 1.80 (2 H _{<i>meta</i>} vs. <i>t</i> Bu) 1.18 (2 H _{<i>ortho</i>} vs. CF ₃) 1.01 (2 H _{<i>ortho</i>} vs. <i>t</i> Bu)	2.86 (3 F)	3.18 (3 F)
2- <i>t</i> Bu-4'-CF ₃	2.00611	9.70	10.01	2.61 (2 H) 0.92 (2 H) 0.63 (1 H) 0.48 (1 H) 0.43 (1 H) 0.24 (1 H)	2.91 (2 H _{<i>ortho</i>}) 1.37 (2 H _{<i>meta</i>}) 0.51 (1 H _{<i>meta</i>}) 0.43 (1 H _{<i>meta</i>}) 0.40 (1 H _{<i>ortho</i>}) 0.28 (1 H _{<i>para</i>})	3.74 (3 F)	3.87 (3 F)
4- <i>t</i> Bu-2'-CF ₃	2.00607	10.02	9.69	2.52 (2 H) 0.85 (2 H) 0.4 (1 H)	2.56 (2 H _{<i>ortho</i>}) 1.23 (2 H _{<i>meta</i>}) 0.97 (1 H _{<i>ortho</i>}) 0.95 (1 H _{<i>para</i>}) 0.72 (1 H _{<i>meta</i>}) 0.70 (1 H _{<i>meta</i>})	0.63 (3 F)	0.33 (3 F)
4-CF ₃ -2'-CF ₃	2.00610	9.39	9.12	2.57 (2 H) 1.05 (2 H) 0.51 (1 H) 0.40 (1 H) 0.44 (1 H) 0.49 (1 H)	2.69 (2 H _{<i>ortho</i>}) 1.29 (2 H _{<i>meta</i>}) 0.23 (1 H _{<i>ortho</i>}) 0.20 (1 H _{<i>meta</i>}) 0.19 (1 H _{<i>meta</i>}) 0.19 (1 H _{<i>para</i>})	3.43 (3 F) 0.16 (3 F)	3.60 (3 F) 0.36 (3 F)
H ₂ H ^[a]	2.0055	9.66		1.83 0.79			
H ₂ H ^[b]	2.0055	9.77		1.83 1.86 0.87			

[a] In xylene, see ref.^[18] [b] Imbedded in a benzophenone single crystal, see ref.^[31]

spectively) though the steric bulkiness for both compounds attributed to the same *ortho*-*t*Bu group might be expected to be similar.

The comparison of the $a(F)$ values for the *ortho*-CF₃ group in 2,4'-bis(trifluoromethylphenyl)nitroxide and 2-CF₃,4'-*t*Bu-diphenylnitroxide shows that the values are significantly different (0.16 G and 0.63 G) in spite of the similar bulkiness, thus indicating the influence of the electronic effects. The combined influence of the electronic effects and steric bulkiness in the series of the twisted nitroxides can be deduced from the comparison of the torsion angle values between the phenyl ring and the N–O plane, which are given in Table 3.

Table 3. DFT-calculated O–N–C torsion angles in the series of the twisted nitroxides (R¹C₆H₄)(R²C₆H₄)NO and standard Gibbs free energies for the unwanted dimerization through the phenyl ring (Scheme 2).

Compound number	Substituents on phenyl rings		C–C–N–O torsion angle, degrees
	R ¹	R ²	
2	<i>o</i> - <i>t</i> Bu	<i>p</i> - <i>t</i> Bu	67.4
3	<i>o</i> - <i>t</i> Bu	<i>o</i> - <i>t</i> Bu	45.3
5	<i>o</i> -CF ₃	<i>p</i> -CF ₃	59.9
6	<i>o</i> -CF ₃	<i>p</i> - <i>t</i> Bu	52.2
7	<i>o</i> - <i>t</i> Bu	<i>p</i> -CF ₃	69.8

The calculated torsion-angle values nicely correlate with the spin density at the carbon atoms taken from the ORCA output. The linear plots between the $\cos \theta$ and the Mulliken spin population at the carbon atoms in the *para*-position of the twisted ring as well as of the integrated spin density over the whole *ortho*-substituted ring are given in Figure 2. The Newman projection given in the inset illustrates the π – π overlap between the NO group and the twisted aryl moiety controlling spin delocalization over the *ortho*-substituted ring.

UV/VIS

UV/Vis spectra for two sets of new isomeric diarylnitroxides are shown in Figure 3. The wavelengths (λ_{\max}) and the molar extinction coefficients (ϵ) are summarized in Table SI-8. All the samples exhibit an intensive peak at 200 nm, a broad intensive peak around 300 nm, and a set of much less intensive peaks in 430–530 nm region. The most interesting is the weak absorption peak in the visible region since it is mainly associated with free-radical electrons located in the SOMOs. The λ_{\max} for the absorption in visible region for diarylnitroxides (430–530 nm) is red-shifted as compared to λ_{\max} for alkyl derivatives (428–468 nm);^[32] the ϵ values are significantly higher for aromatic than for aliphatic (ϵ 4–10) compounds due to spin delocalization. The minimal extinction among the set of compounds given in Figure 3 is observed for the *ortho*-*t*Bu, *para*-CF₃ derivative which exhibits the largest O–N–C–C dihedral angle (see Table 3). The interpretation of the wavelengths values observed within the series of nitroxides given in Table 3 is not trivial since the SOMO energy is influenced by the different trends, including the bulkiness of the molecule and electron effects of the substituents. The latter are dependent not only on the nature of the addends but on the conjugation degree as well.

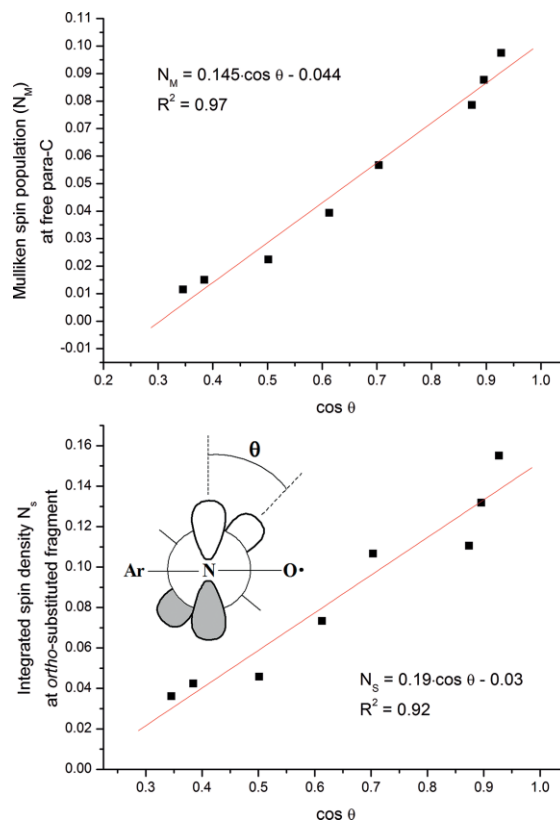


Figure 2. The Mulliken spin population at the carbon atoms in *para*-position of the twisted ring vs. $\cos \theta$ linear fit (a) and the integrated spin density over the whole *ortho*-substituted ring vs. $\cos \theta$ linear fit (b). The Newman projection illustrates the π – π overlap between the NO group and the twisted aryl moiety. Points for two 4,4'-substituted nitroxides **1** and **4** are also included.

Stability Tests

The idea that removing the aryl moiety from the conjugation plane with the nitroxyl radical center, and thus preventing spin density delocalization over the phenyl ring, will drastically increase the stability of the radical was supported by the ESR data.

The radicals are highly stable. In crystalline form, they can be kept for months in air without any noticeable degradation. For quantitative estimation of the radical life time, a spin-counting method was applied. Thus, the sample of 2-*t*Bu,4'-CF₃-diphenylnitroxide was kept in a benzene solution for more than two weeks in air at room temperature without protection from light. The amount of radical species that was exhibited was 100 % of the starting value. The isomeric 2-CF₃,4'-*t*Bu-diphenylnitroxide is comparably less stable; after 7 d in toluene solution in air at room temperature the amount of radical species exhibited by the sample was 85 % of the starting value. This decrease in stability might be attributed to more significant spin delocalization over the phenyl ring, as follows from the comparison of the calculated O–N–C–C torsion angle and the $a(N)$ *hfcc* values for these two isomers (see Table 2 and Table 3). Interestingly, the nitroxides are relatively stable even in halogenated solvents (such as CHCl₃). Thus, the NMR sample of 2,4'-bis(*tert*-butylphenyl)nitroxide in CDCl₃ stayed unchanged for more than 30 h without light protection. For comparison, previously re-

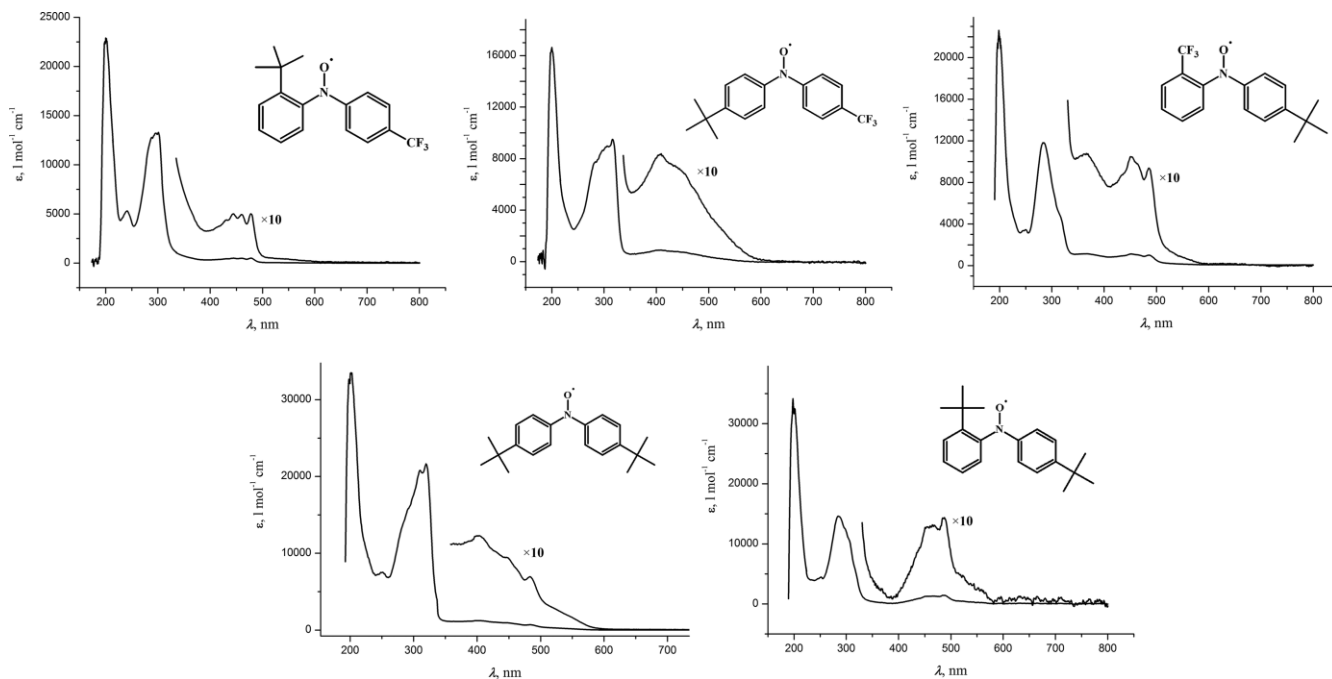


Figure 3. UV/Vis spectra for two sets of new isomeric diarylnitroxides.

ported^[33] comparably stable bridged diarylnitroxides decomposed in CHCl_3 solution under solar irradiation in 12 min.

To quantify stability of the radicals and to demonstrate the role of twisting in their stabilization, kinetic measurements in toluene were performed. The experiments in toluene are important since they allow an estimation of the inherent stability of the radicals toward decomposition contrary to the experiments in chloroform. The latter is known to produce the radicals, which can initiate secondary radical transformations, whereas the H-donor abilities of both solvents are similar. Since the radicals are stable in solution under solar irradiation, harsher irradiation (laser light, wavelength 405 nm, intensity 5×10^{-9} Einstein/s per sample) were applied to get reliable quantitative data. ESR spectra of two isomeric 2,4'- and 4,4'-bis(*tert*-butylphenyl)nitroxides were recorded in the course of irradiation, and quantum yields of photochemical decomposition were determined.

The following kinetic model of photochemical radical decomposition was used:

$$\frac{dN}{dt} = I_0[1 - 10^{-A(t)}]\varphi$$

where N is the number of radical molecules, I_0 is light intensity, φ is the quantum yield of the reaction, $A(t)$ is the absorbance of the solution at the irradiation wavelength [calculated by Bouguer–Lambert–Beer's law $A(t) = \frac{\epsilon_{405}l}{V}N(t)$ where ϵ_{405} is extinction coefficient on the irradiation wavelength, l is the optical path length of irradiating light, and V is the sample volume].

The value of $I_0[1 - 10^{-A(t)}]$ is the number of photons absorbed by radical molecules per unit time, and the expression $\Delta(t) = \int_0^t I_0[1 - 10^{-A(\tau)}]d\tau$ represents the absorbed irradiation dose. Accordingly, the slope of the linear dependence of $N(t)$ vs. $\Delta(t)$ gives the quantum yield of photochemical decomposi-

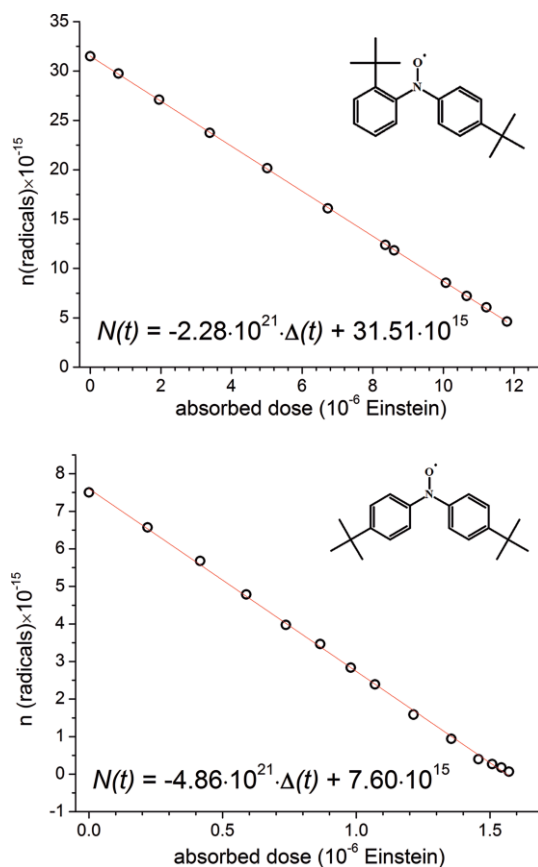


Figure 4. Stability tests under laser irradiation.

tion of the radicals. The results obtained for isomeric 2,4'- and 4,4'-bis(*tert*-butylphenyl)nitroxides are given in Figure 4. The quantum yields of the photochemical decomposition measured

as described are $(8 \pm 2) \times 10^{-3}$ for 4,4'-substituted radical and $(4 \pm 1) \times 10^{-3}$ for the 2,4'-isomer. The results obtained clearly indicate the increased stability of the twisted isomer as compared to the planar one.

HRMS analyses of the solutions obtained after irradiation of the radicals were performed. These revealed the formation of corresponding amines and a certain amount of O-arylated diarylnitroxides. The analog of the latter product (O-alkylated nitroxide) was also detected among the products of photochemical destruction of stable di-*tert*-butylnitroxide.^[34] A detailed analysis of the possible photochemical decay channels for all new diarylnitroxides is in currently progress and will be the subject of a forthcoming paper.

Conclusions

The main problem of decreasing stability of diarylnitroxides as compared to the aliphatic analogs is spin-density delocalization over the phenyl ring, which provokes various radical transformations. A new strategy for the molecular design of stable diarylnitroxides was elaborated based on the insertion of a bulky substituent into the *ortho*-position of the phenyl ring, thus disturbing its conjugation with the radical center. A series of twisted diarylnitroxides with *tert*-butyl and trifluoromethyl substituents in different positions and combinations was obtained and fully characterized with HRMS, ESR, and UV/Vis methods. The compounds are stable in the solid state and in solution. These nitroxides constitute the first examples of stable diarylnitroxides with a vacant *para*-position on the phenyl ring. ESR and DFT studies confirmed that the *ortho*-substituted phenyl ring is removed from the conjugation with the NO radical center. Comparative ESR investigations of the isomeric 4,4'-, 2,4'-, and 2,2'-bis(*tert*-butylphenyl)nitroxides indicated significant difference in the spin-splitting constants. The maximal *hfcc* value with the ¹⁴N nucleus is observed in the case of the 2,2'-isomer, which indicates poor delocalization of the spin density over both phenyl rings.

It was shown that the O–N–C–C torsion angle is dependent not only on the bulkiness of the *ortho*-substituent, but it is also influenced by the electron-donating or electron-withdrawing ability of the substituents in both phenyl rings. The presence of the strong electron-withdrawing group on one phenyl ring facilitates delocalization of the nitrogen lone pair over the ring; thus, the necessity for the conjugation of the NO moiety with the other ring is decreased, and the *ortho*-substituted ring is more prone to be twisted out of the plane according to the steric demands of the *ortho*- group.

This approach will broaden the availability of practically important stable nitroxides.

Experimental Section

General Information: Mass spectra were measured with a high-resolution time-of-flight instrument by using electrospray ionization (ESI-MS)^[20]. Measurements were performed in positive ion mode with an interface capillary voltage at 4.5 kV, an effective scan range at *m/z* 100–1200, external calibration (0.016 M sodium formate in

MeCN/water, 1:1 mixture or ESI-L Low Concentration Tuning Mix, Agilent Technologies), direct syringe injection at flow rate of 3 μ L/min, nitrogen as dry gas at 4 L/min, and interface temperature at 180 °C.

ESR spectra were recorded from toluene solutions containing approximately 5×10^{15} radical molecules, which were deaerated by using standard freeze-pump-thaw techniques.

UV/Vis spectra were recorded from solutions of the nitroxides in dry acetonitrile (5×10^{-5} – 1×10^{-4} M).

¹H (400.0) MHz NMR spectra were recorded in CDCl₃. Chemical shifts were referenced to signals from residual non-deuterated solvents.

Computational Details: Stationary-point structure search for all the radicals as well as vibrational analysis for the structures obtained was performed in PRIRODA quantum-chemistry program.^[35,36] The gradient-corrected exchange-correlation Perdew, Burke, and Ernzerhof (PBE) functional^[37] and basis sets L1 were used for calculations.^[38] The 10^{-6} threshold on the molecular gradient at the geometry optimization procedure was employed. Integration of spin density over *ortho*-substituted aromatic moiety basin was performed in Multiwfn program.^[39] The region of integration was defined as the combination of Bader's atomic basins of C and H atoms of the *ortho*-substituted ring and all atoms of the *ortho*-substituent.

ESR spectra were calculated in ORCA 3.0 quantum chemistry program^[40] for gas phase optimized geometries at B1LYP/cc-pVDZ level with SMD solvation model.^[41] RIJCOSX^[42] approximation was employed.

Oxidation to Nitroxides. 2,4'-Bis(*tert*-butylphenyl)nitroxide (Method a): A solution of 281 mg (1.0 mmol) of unsymmetrical 2,4'-bis(*tert*-butylphenyl)amine in 5 mL of methanol was heated to the boiling point. Afterwards, 340 μ L (3.0 mmol) of 30 % hydrogen peroxide and a solution of 33 mg (0.1 mmol) of Na₂WO₄·2H₂O in 70 μ L of water were successively added, and the mixture was heated under reflux for 12 h. Portions of hydrogen peroxide (340 μ L) were added every 3 h. The consumption of diarylamine was monitored by TLC (eluent – toluene/hexane, 1:10). After all starting material was consumed, the reaction mixture was cooled, diluted with water, and extracted with diethyl ether. Organic fractions were washed with water, dried with sodium sulfate, and purified by column chromatography on silica gel (eluent – toluene, *R_f* = 0.44). The nitroxide was obtained as reddish-orange oil (133 mg, 45 % yield). ESI-HRMS: *m/z* 296.2012 (M⁺, 296.2009 calculated for C₂₀H₂₆NO), 297.2078 (M + H⁺, 297.2087 calculated for C₂₀H₂₇NO). λ_{max} , nm: 538 (sh), 487, 465, 302 (sh), 285, 251, 200.

2,4'-Bis(*tert*-butylphenyl)nitroxide (Method b): To a solution of 50 mg (0.18 mmol) of unsymmetrical 2,4'-bis(*tert*-butylphenyl)amine in 1.5 mL of ether cooled to –15 °C, a solution of 46 mg (0.29 mmol) of *m*CPBA in 1 mL of ether was added. The mixture was kept at –15 °C for 10 min and afterwards at room temperature for 2 h. The color of solution gradually changed to dark red. The mixture was quenched with water, washed with saturated aqueous NaHCO₃, dried with Na₂SO₄, the solvent was evaporated, and the product purified by column chromatography on silica gel by using toluene as an eluent; 10 mg (19 %) of the nitroxide was obtained.

2,2'-Bis(*tert*-butylphenyl)nitroxide: A solution of 28 mg (117 μ mol) of *m*-chloroperbenzoic acid in 3 mL of diethyl ether was added to a solution of 30 mg of 2,2'-bis(*tert*-butylphenyl)amine in 6 mL of diethyl ether. The mixture was kept in the dark for 5 d at room temperature. The resulting pale-red solution was evaporated,

and the residue was washed with toluene on glass filter. The toluene solution was concentrated and purified by column chromatography on silica gel by using toluene as eluent. 2,2'-bis(*tert*-butylphenyl)nitroxide was isolated in 10 % yield as a red solid. ESI-HRMS: m/z 296.2010 (M^+ , 296.2009 calculated for $C_{20}H_{26}NO$), 297.2081 ($M + H^+$, 297.2087 calculated for $C_{20}H_{27}NO$).

4-(Trifluoromethylphenyl)-4'-(*tert*-butylphenyl)nitroxide: A solution of 200 mg (0.68 mmol) of 4-(trifluoromethyl)-4'-*tert*-butyldiphenylamine in 5 mL of methanol was heated to the boiling point. Afterwards, 230 μ L (2.2 mmol) of 30 % hydrogen peroxide and a solution of 22 mg (0.07 mmol) of $Na_2WO_4 \cdot 2H_2O$ in minimal volume of water were successively added. The mixture was heated under reflux for 12 h. Portions of hydrogen peroxide (230 μ L in 1.3 mL of MeOH) were added every 5 h. After 15 h of refluxing, the reaction mixture was diluted with CH_2Cl_2 (20 mL), washed with water, dried with Na_2SO_4 , and the solvent was evaporated under reduced pressure. The residue was purified by column chromatography on silica gel by using a 1:1 mixture of toluene/hexane as eluent. After evaporation of the colored fraction, 30 mg of the targeted nitroxide was obtained. 100 mg of the starting amine was also recovered from the preceding colorless fraction. ESI-HRMS: m/z 308.1262 (M^+ , 308.1262 calculated for $C_{17}H_{17}F_3NO$). λ_{max} , nm: 518 (sh), 450 (sh), 408, 316, 306, 295, 281, 199.

2-(Trifluoromethylphenyl)-4'-(*tert*-butylphenyl)nitroxide: 100 mg (0.34 mmol) of 2-*tert*-butyl-4'-(trifluoromethyl)diphenylamine was dissolved in 2 mL of $CHCl_3$. A solution of 140 mg (0.57 mmol) of 70 % mCPBA in 2 mL of $CHCl_3$ was added. The reaction mixture was kept at room temperature for 3 h, diluted with $CHCl_3$ (10 mL), washed with Na_2CO_3 solution, dried with Na_2SO_4 , and the solvent was evaporated under reduced pressure. The residue was purified by column chromatography on silica gel (with CH_2Cl_2 /hexane, 1:1 as an eluent). The second colored fraction was collected and evaporated yielding 33 mg (31 %) of the targeted nitroxide as a brownish-yellow oil. ESI-HRMS: m/z 308.1262 (M^+ , 308.1262 calculated for $C_{17}H_{17}F_3NO$). λ_{max} , nm: 534 (sh), 485, 463 (sh), 452, 434 (sh), 366, 314 (sh), 284, 247, 199.

4-(Trifluoromethylphenyl)-2'-(*tert*-butylphenyl)nitroxide: 100 mg (0.34 mmol) of 2-*tert*-butyl-4'-(trifluoromethyl)diphenylamine was dissolved in 2 mL of $CHCl_3$. A solution of 140 mg (0.57 mmol) of 70 % mCPBA in 2 mL of $CHCl_3$ was added. The resulting solution was kept at room temperature for 3 h, diluted with $CHCl_3$ (10 mL), washed with Na_2CO_3 solution, dried with Na_2SO_4 , and the solvent was evaporated under reduced pressure. The residue was purified by column chromatography on silica gel (with CH_2Cl_2 /hexane, 1:2 as an eluent). The first colored fraction was collected and evaporated yielding 43 mg (41 %) of the targeted nitroxide as a brownish-orange oil. ESI-HRMS: m/z 308.1260 (M^+ , 308.1262 calculated for $C_{17}H_{17}F_3NO$), ESI-HRMS: m/z 309.1339 ($M + H^+$, 309.1335 calculated for $C_{17}H_{18}F_3NO$). λ_{max} , nm: 531 (sh), 477, 460, 443, 430, 413 (sh), 301, 295, 288, 240, 200.

2,4'-Bis(trifluoromethylphenyl)nitroxide: 150 mg (0.49 mmol) of 2,4'-bis(trifluoromethyl)diphenylamine was dissolved in 5 mL of $CHCl_3$. A solution of 140 mg (0.57 mmol) of 70 % mCPBA in 5 mL of $CHCl_3$ was added. The resulting solution was heated to 40 $^{\circ}C$, kept at this temperature for 5 h and left overnight at room temperature. The resulting solution was diluted with $CHCl_3$ (10 mL), washed with Na_2CO_3 solution, dried with Na_2SO_4 and the solvent was evaporated under reduced pressure. The residue was purified by column chromatography on silica gel with a 8:1 mixture of hexane/ethyl acetate as eluent. The second colored fraction was collected and evaporated yielding 39 mg (25 %) of the targeted nitroxide as a

brownish-orange oil. ESI-HRMS: m/z 320.0504 (M^+ , 320.0510 calculated for $C_{14}H_8F_6NO$).

Supporting Information (see footnote on the first page of this article): ESI-HRMS spectra, HPLC-MS, and 1H NMR spectroscopic data are available.

Acknowledgments

This work was supported by Russian Science Foundation (Project number 16-13-10282). NMR parts of this work were supported by Lomonosov Moscow State University "Program of Development".

Keywords: Radicals · Nitroxides · ESR · Conjugation · Oxidation

- [1] H. Karoui, F. Le Moigne, O. Ouari, P. Tordo, in *Stable Radicals Fundam. Appl. Asp. Odd-Electron Compd.* (Ed. R. G. Hicks), John Wiley & Sons Ltd, Chichester, West Sussex, **2010**, pp. 173–230.
- [2] G. I. Likhtenshtein, J. Yamauchi, S. Nakatsuji, A. I. Smirnov, R. Tamura, *Nitroxides. Applications in Chemistry, Biomedicine, and Materials Science*, WILEY-VCH Verlag GmbH & Co. KGaA, Weinheim, **2008**.
- [3] S. Goldstein, A. Samuni, K. Hideg, G. Merenyi, *J. Phys. Chem. A* **2006**, *110*, 3679–3685.
- [4] J. L. Hodgson, M. Namazian, S. E. Bottle, M. L. Coote, *J. Phys. Chem. A* **2007**, *111*, 13595–13605.
- [5] S. Goldstein, G. Merenyi, A. Russo, A. Samuni, *J. Am. Chem. Soc.* **2003**, *125*, 789–795.
- [6] B. P. Soule, F. Hyodo, K. Matsumoto, N. L. Simone, J. A. Cook, M. C. Krishna, J. B. Mitchell, *Free Radical Biol. Med.* **2007**, *42*, 1632–1650.
- [7] K. Nakahara, S. Iwasa, M. Satoh, Y. Morioka, J. Iriyama, M. Suguro, E. Hasegawa, *Chem. Phys. Lett.* **2002**, *359*, 351–354.
- [8] H. Nishide, S. Iwasa, Y.-J. Pu, T. Suga, K. Nakahara, M. Satoh, *Electrochim. Acta* **2004**, *50*, 827–831.
- [9] H. Nishide, K. Oyaizu, *Science* **2008**, *319*, 737–738.
- [10] K. Nakahara, K. Oyaizu, H. Nishide, *Chem. Lett.* **2011**, *40*, 222–227.
- [11] C. J. Hawker, A. W. Bosman, E. Harth, *Chem. Rev.* **2001**, *101*, 3661–3688.
- [12] A. Nilsen, R. Braslau, *J. Polym. Sci., Part A J. Polym. Sci., Part A Polym. Chem.* **2006**, *44*, 697–717.
- [13] R. A. Sheldon, I. W. C. E. Arends, *Adv. Synth. Catal.* **2004**, *346*, 1051–1071.
- [14] T. Vogler, A. Studer, *Synthesis* **2008**, 1979–1993.
- [15] J. M. Bobbitt, C. Brückner, N. Merbouh, in *Organic Reactions*, John Wiley & Sons, Inc. **2004**.
- [16] R. Ciriminna, M. Pagliaro, *Org. Process Res. Dev.* **2010**, *14*, 245–251.
- [17] L. Tebben, A. Studer, *Angew. Chem. Int. Ed.* **2011**, *50*, 5034–5068; *Angew. Chem.* **2011**, *123*, 5138.
- [18] P. H. H. Fischer, F. A. Neugebauer, *Z. Naturforsch. A* **1964**, *19*, 1514–1517.
- [19] M. Ballester, J. Riera, C. Onrubia, *Tetrahedron Lett.* **1976**, *17*, 945–946.
- [20] Y. A. Ivanov, A. I. Kokorin, A. B. Shapiro, E. G. Rozantsev, *Bull. Acad. Sci. USSR Div. Chem. Sci. (Engl. Transl.)* **1976**, *25*, 2069.
- [21] T. Ishida, M. Nakagawa, R. Imachi, Y. Akui, S.-Y. Masaoka, M. Suzuki, D. Hashizume, Masanoriyasui, F. Iwasaki, T. Nogami, *Mol. Cryst. Liq. Cryst.* **1999**, *334*, 89–98.
- [22] A. Calder, A. R. Forrester, *J. Chem. Soc. C* **1969**, 1459–1464.
- [23] K. Itoh, M. Kinoshita (Eds.), *Molecular Magnetism, New Magnetic Materials*, Gordon & Breach Science Publishers, Amsterdam, **2000**.
- [24] A. Rajca, M. Vale, S. Rajca, *J. Am. Chem. Soc.* **2008**, *130*, 9099–9105.
- [25] A. Rajca, K. Shiraiishi, S. Rajca, *Chem. Commun.* **2009**, *3*, 4372–4374.
- [26] A. Rajca, M. Takahashi, M. Pink, G. Spagnol, S. Rajca, *J. Am. Chem. Soc.* **2007**, *129*, 10159–10170.
- [27] T. Suga, H. Nishide, in *Stable Radicals Fundam. Appl. Asp. Odd-Electron Compd.* (Ed. R. G. Hicks), John Wiley & Sons Ltd, Chichester, West Sussex, **2010**, pp. 507–520.
- [28] T. Magdesieva, O. Levitskiy, Y. Grishin, V. Sentyurin, *Chem. Eur. J.*, <https://doi.org/10.1002/chem.201702270>.
- [29] V. A. Golubev, V. D. Sen', *Russ. J. Org. Chem.* **2013**, *49*, 555–558.

- [30] A. Zakrassov, M. Kaftory, *J. Solid State Chem.* **2002**, *169*, 75–80.
[31] T.-S. Lin, *J. Chem. Phys.* **1972**, *57*, 2260.
[32] K. Nakahara, S. Iwasa, J. Iriyama, Y. Morioka, M. Suguro, M. Satoh, E. J. Cairns, *Electrochim. Acta* **2006**, *52*, 921–927.
[33] R. Suzuki, R. Tada, Y. Miura, N. Yoshioka, *J. Mol. Struct.* **2016**, *1106*, 399–406.
[34] D. R. Anderson, T. H. Koch, *Tetrahedron Lett.* **1977**, *35*, 3015–3018.
[35] D. N. Laikov, Y. A. Ustynyuk, *Russ. Chem. Bull.* **2005**, *54*, 820–826.
[36] D. N. Laikov, *Chem. Phys. Lett.* **1997**, *281*, 151–156.
[37] J. P. Perdew, K. Burke, M. Ernzerhof, *Phys. Rev. Lett.* **1997**, *78*, 1396.
[38] D. N. Laikov, *Chem. Phys. Lett.* **2005**, *416*, 116–120.
[39] T. Lu, F. Chen, *J. Comput. Chem.* **2012**, *33*, 580–592.
[40] F. Neese, *Wiley Interdiscip. Rev. Comput. Mol. Sci.* **2012**, *2*, 73–78.
[41] A. V. Marenich, C. J. Cramer, D. G. Truhlar, *J. Phys. Chem. B* **2009**, *113*, 6378–6396.
[42] F. Neese, F. Wennmohs, A. Hansen, U. Becker, *Chem. Phys.* **2009**, *356*, 98–109.

Received: July 7, 2017